2012-12-28

Adsorption and Electrooxidation of Carbon Monoxide on Platinum Surfaces Modified with Sulfur

A. Mattox Mathew

W. Henney Matthew

Johnson Adam

Zou Shouzhong
Department of Chemistry & Biochemistry, Miami University, Oxford, OH 45056, USA;, zous@muohio.edu

Adsorption and Electrooxidation of Carbon Monoxide on Platinum Surfaces Modified with Sulfur

Mathew A. Mattox, Matthew W. Henney, Adam Johnson, Shouzhong Zou*

(*Department of Chemistry & Biochemistry, Miami University, Oxford, OH 45056, USA*)

Abstract:　　Adsorbed sulfur is commonly considered as a reaction poison. However, small amounts of sulfur on platinum significantly increase the surface reactivity toward carbon monoxide (CO) electrooxidation. For the solution CO oxidation, the onset potential was shifted up to over 300 mV negative to that on S-free surface, and the extent of the negative potential shift increases with the sulfur coverage (X_S) up to about 0.6. The enhanced CO oxidation also depends on the solution pH. For the adsorbed CO, at low sulfur coverages ($X_S < 0.3$), the oxidation peak potential is about 40 mV negative to that of the corresponding clean Pt. However, at higher coverages, the peak potential is about 30 mV more positive. Surface-enhanced Raman spectra show that the adsorption of sulfur significantly redshifts the Pt—CO stretching frequency. These observations are explained by the weakening of the Pt—CO bond and the hindrance of CO diffusion by S_{ads}.

Key words:　　electrooxidation; adsorbed sulfur; carbon monoxide; platinum; surface-enhanced Raman spectroscopy

CLC Number:　　O646　　　　　　　　　**Document Code:**　　A

1　Introduction

The adsorption of foreign atoms can significantly modify the chemical and physical properties of a metal surface, thereby changes the surface reactivity[1]. Depending on the nature of the adatom and the reaction, the adatom can be either a reaction promoter or a reaction poison. Adsorbed sulfur is commonly regarded as a reaction poison for both gas phase and electrochemical reactions[1-14]. In gas phase reactions, the adsorbed sulfur is known to reduce the reactivity of Pt toward small molecules, such as carbon monoxide (CO)[2-8,14]. In electro-chemical systems, adsorbed sulfur blocks the hydrogen adsorption and evolution[9-13,15]. To understand the sulfur poisoning effect, extensive experimental and theoretical studies have been conducted, mostly in the ultra high vacuum[2-8, 14, 16-19]. The likely effects of adsorbed sulfur, though not completely agreed upon, include modification of the electronic structure of the surface, such as lowering the metal d band occupancy; physically blocking certain surface sites therefore changing the reaction pathway (the so-called third body effect); and direct interaction with reactants through electrostatic interactions[2-8, 14, 16-19]. These effects can be either long or short range.

On the contrary to the common perception that adsorbed sulfur is a surface poison, there are several reactions in which a catalytic effect has been observed[20-25]. In the late 1960s, Binder et al. first reported the electrooxidation of solution CO (i.e. CO dissolved in solution) and formic acid on Raney Pt was promoted by sulfur[20-21]. Soon after this, Loucka observed the enhancement of methanol oxidation on Pt by adsorbed sulfur[25]. In 1985, Watanabe and Motoo reported detailed studies of the sulfur enhancement effect on CO oxidation by varying the sulfur coverage and solution pH[23-24]. Very recently, it was shown that on carbon supported

Pt nanoparticles (Pt/C) the oxidation of the irreversibly adsorbed CO was also enhanced by coadsorbed sulfur [26]. However, a satisfactory account of the sulfur enhancement effect is lacking. Given the importance of CO and methanol electro-oxidation in methanol fuel cells and the widespread interest in understanding the sulfur effects on surface reactions, it is worthwhile to further study the mechanism dictating the observed peculiar enhancement effect.

Herein we report results from cyclic voltammetric and chronoamperometric studies of the electro-oxidation of CO on Pt surfaces modified with sub-monolayer of sulfur. The effects of sulfur coverage and solution pH on solution CO oxidation were examined. While the results confirm the enhancement effect of adsorbed sulfur (S_{ads}) on solution CO oxidation, some significant differences w ere also observed. The influence of S_{ads} on the oxidation of irreversibly adsorbed CO is more complicated. At low sulfur coverages, the CO oxidation potential is more negative than on the S-free Pt; while at high sulfur coverages, it is more positive. Surface-enhanced Raman spectroscopy provides new insights into the mechanism of the S promotion effect on the CO oxidation by probing the adsorbed sulfur induced Pt—CO bond change and the modification of CO adlayer structure. This study shows that the observed effects of S_{ads} on the solution phase and adsorbed CO oxidation can be understood by the weakening of the Pt—CO bond and the hindrance of CO_{ads} diffusion by S_{ads}.

2　Experimental

2.1　Chemicals

The 0.1 mol · L^{-1} HClO$_4$ was prepared from double distilled 70% perchloric acid (HClO$_4$) obtained from GFS Chemicals (Powell, OH). Semiconductor grade (99.997%) carbon monoxide (CO) was procured from Spectra Gas (Branchburg, NJ). Other reagents are of analytical or highergrade. Sodium perchlorate (NaClO$_4$) was from Fluka (St. Louis, MO). Sodium hydroxide (NaOH), glacial

acetic acid (CH$_3$COOH), boric acid (H$_3$BO$_3$), and sodium sulfide (Na$_2$S) were obtained from Fisher Scientific (Hampton, NH). Na$_2$S was recrystallized twice in milli-Q water prior to use. Sodium hydrogenphosphate (Na$_2$HPO$_4$) and sodium dihydro-genphosphate (NaH$_2$PO$_4$) were obtained from Sigma-Aldrich (St. Louis, MO). Solutions were made using Milli-Q water (18.2 MΩ · cm resistivity, Milli-Q Synthesis A10, Millipore, Billerica, MA).

For experiments conducted at different pHs, the electrolyte pH was controlled by using 0.1 mol · L^{-1} HClO$_4$, 0.1 mol · L^{-1} NaOH, and different buffers. The pH 1 experiments were conducted in 0.1 mol · L^{-1} HClO$_4$. The pH 3 solution was prepared by acidify-ing 0.1 mol · L^{-1} NaClO$_4$ through dropwise addition of 0.1 mol · L^{-1} HClO$_4$. The pH 5 experiments were conducted in an aqueous buffer solution containing 10 mmol · L^{-1} glacial acetic acid and 90 mmol · L^{-1} NaClO$_4$, adjusted to pH 5 with 1 mol · L^{-1} NaOH. The pH 7 solution contains 5 mmol · L^{-1} NaH$_2$PO$_4$, 5 mmol · L^{-1} Na$_2$HPO$_4$ and 90 mmol · L^{-1} NaClO$_4$. The pH 9 solution was 10 mmol · L^{-1} boric acid and 90 mmol · L^{-1} NaClO$_4$ adjusted to the pH by addition of 1 mol · L^{-1} NaOH. The pH 12 experiments were con-ducted in 0.1 mol · L^{-1} NaOH.

2.2　Electrochemical Measurements

Cyclic voltammograms and chronoamperomet-ric plots were obtained using a conventional two-compartment, three electrode cell consisting of a Pt wire counter electrode and a Ag/AgCl reference electrode (CH Instruments, Austin, TX). A Pt disk with a diameter of 2 mm from CH Instruments was used as the working electrode. Prior to each mea-surement, the Pt working electrode was polished successively with 1.0 and 0.3 μm Al$_2$O$_3$ powder on a polishing cloth (Buehler, Lake Bluff, IL). The elec-trode was then sonicated in water for 10 min and rinsed with water to remove any residual powder. The electrode was further cleaned by cycling the ap-plied electrode potential between -0.25 and 0.8 V in CO saturated 0.1 mol · L^{-1} HClO$_4$ and followed by stripping off the irreversibly adsorbed CO in N$_2$ purged 0.1 mol · L^{-1} HClO$_4$. CH Instruments Model

630 electrochemical analyzer was used for all of the electrochemical experiments. All of the measurements were conducted at room temperature (23 ± 1)°C.

2.3 Surface-Enhanced Raman Specroscopy (SERS)

To obtain surface enhanced Raman effect on Pt, the overlayer method was used[27-30]. Briefly, a Au electrode was polished successively with 1.0 and 0.3 μm Al_2O_3 powder on a polishing cloth and roughened by electrochemical oxidation-reduction cycles in 0.1 mol·L^{-1} KCl to obtain SERS activity as described by Gao et al[31]. Platinum thin films were electrodeposited on the SERS active Au surface by the redox replacement approach[32]. To ensure the Au surface is entirely covered by Pt, 2 to 3 redox replacement cycles were employed[32]. Raman spectra were collected with a micro-Raman probe (Spectra-Code, West Lafayette, IN) equipped with a SpectraPro300i triple grating monochromator (Acton Research, Acton, MA) and a liquid nitrogen cooled red-intensified back illumination CCD detector (Princeton Instruments, Trenton, NJ). The laser excitation at 785 nm was from a diode laser (Process Instruments, Salt Lake City, UT) coupled to optical fiber bundles and focused onto the sample with a long working distance 20 × microscope objective (NA 0.42) to a 100 μm spot. The Raman scattering light was collected in a back-scattering fashion with the same objective. The laser power at the sample was around 5 mW. The Raman shift axis was calibrated with a neon light. Typical spectrum acquisition time was 30 s.

3 Results

3.1 Cyclic Voltammogram of Sulfur-Covered Pt

Before presenting the results for CO oxidation, it is helpful to first show the electrochemical response of the sulfur-covered Pt electrodes in a potential range where CO oxidation occurs. Displayed in Fig. 1 is a set of cyclic voltammograms for sulfur covered Pt with various coverages obtained in 0.1 mol·L^{-1} $HClO_4$. The current density was calculated using the surface area of the clean Pt, which was evaluated by the hydrogen desorption charge assuming the charge density is 210 μC·cm^{-2} for desorption of a full monolayer of adsorbed hydrogen (H_{ads})[13]. Before sulfur adsorption, the electrode was cleaned by cycling the applied potential between -0.25 and 0.8 V in CO-saturated 0.1 mol·L^{-1} $HClO_4$ and followed by stripping off the irreversibly adsorbed CO in N_2-purged 0.1 mol·L^{-1} $HClO_4$. The sulfur adlayer was formed by holding the electrode at -0.6 V in y mmol·L^{-1} Na_2S + 0.1 mol·L^{-1} $NaClO_4$ +1 mmol·L^{-1} NaOH for 60 s. To obtain different sulfur coverages, y was varied from 0.01 to 2. Although increasing the sulfide concentration or holding the potential at more positive values can increase the amount of sulfur on the surface, the sulfur coverage achievable by this means is sufficient for our purpose. Further increasing the sulfur coverage will block the solution CO oxidation. More importantly, holding the potential at -0.6 V helps to minimize the formation of polysulfur from the oxidation of sulfide, as indicated by SERS experiments.

Two features are clearly evident in Fig. 1. In the hydrogen adsorption/desorption potential region (-0.25 to 0.1 V), the current decreases with increas-
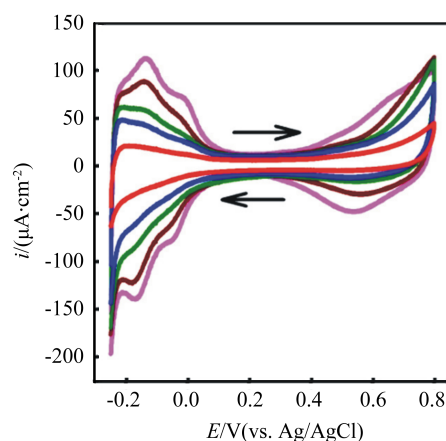

Fig. 1 Cyclic voltammograms of Pt electrodes covered with various amount of sulfur in 0.1 mol·L^{-1} $HClO_4$. The relative sulfur coverage X_S from the outer most trace to the inner most trace is: 0, 0.24, 0.48, 0.63, 0.86. The arrows indicate the scan direction. The scan rate was 0.1 V·s^{-1}.

ing amounts of sulfur on the surface (from the outer most trace to the inner most trace). In the surface oxidation/reduction potential region (0.3 to 0.8 V), the adsorbed sulfur suppresses the formation of Pt oxides and pushes the surface oxidation to higher potentials with increasing sulfur coverage and eventually blocks the oxidation. These observations are consistent with those reported in previous studies of sulfur adsorption on Pt and indicate the adsorbed sulfur (S_{ads}) poisons the hydrogen adsorption and surface oxidation[10, 12-13]. It is noted that the sharp peak observed on Pt(111) at high sulfur coverages was absent in the potential region examined here, probably because the amount of sulfur on the surface is considerably smaller (vide infra) and because of the polycrystalline nature of the surface[12-13]. The cyclic voltammogram for each S-modified Pt electrode is stable upon several potential cycles in the region shown in Fig. 1, indicating there is no desorption or oxidation of S_{ads}.

From the hydrogen adsorption/desorption charge, it is possible to calculate the sulfur coverage. A commonly used approach assumes that one S_{ads} blocks one H_{ads} and the sulfur coverage can be calculated as[21, 23-25]:

$$X_s = \frac{Q_H^0 - Q_H^S}{Q_H^0} \qquad (1)$$

Where Q_H^0 and Q_H^S are the H desorption charge from clean and sulfur-covered Pt surfaces, respectively. In all of the previous studies of CO and methanol oxidation on sulfur-covered Pt surfaces, the sulfur coverage was calculated by using Equation. (1)[21, 23-25]. However, studies on Pt(111) electrodes[9, 10, 12-13] and Pt particles[33] suggest that the number of H_{ads} blocked by a single S_{ads} is not unity, but depends on the sulfur coverage. At low sulfur coverages, it can be as large as ten and decreases with increasing sulfur coverage[9, 10, 12-13]. When the sulfur coverage (θ_S) is about 0.33, the charge from H adsorption/desorption is negligible, suggesting the hydrogen adsorption is nearly completely blocked[9, 10, 12-13].

Another way to measure the coverage of S_{ads} is to use the charge for S_{ads} oxidation to SO_4^{2-}, as shown by Sung et al.[12-13]:

$$\theta_S = \frac{Q_S}{6 \times Q_H^0} \qquad (2)$$

where the Q_S is the charge involved in the S_{ads} oxidation. Recently Park et al. claimed that the adsorbed sulfur species is S^{2-} on the basis of comparing the Pt—S stretching frequency from SERS and that from the quantum calculations[33]. This assertion disagrees with a number of previous studies which show nearly completely charge transfer from S^{2-} to metals upon its adsorption[13, 34-35]. The ratio of X_S to θ_S yields the number of H_{ads} blocked by S_{ads}. The oxidation of S_{ads} on the present polycrystalline Pt occurs at a much higher potential (peaking at around 1 V) than that reported on Pt(111)[12-13] and the oxidation peak is broad (supporting information). S_{ads} was completely removed after 3 to 4 potential cycles between -0.25 and 1.2 V, as indicated by the overlapping of the H adsorption/desorption current at the consecutive cycles. Cyclic voltammetric results show that the θ_S evaluated by using Equation (2) is 2 to 4 times lower than the corresponding X_S, indicating S_{ads} blocks more than one H_{ads}. Therefore X_S is the relative sulfur coverage, i.e. relative to the sulfur coverage at which S_{ads} completely blocks the hydrogen adsorption (CO adsorption as well, vide infra). In contrast to the results from Pt(111) surface[9, 10, 12-13], at lower θ_S the S_{ads} blocks less H_{ads} than at higher θ_S. The maximum θ_S obtained is around 0.3. For θ_S larger than an undetermined value at which the X_S cannot be used, the CO oxidation is completely blocked and is not useful for the purpose of the present work. Therefore in the following, we still use X_S, instead of θ_S, to denote different amount of sulfur on the surface for better comparison with the previous work.

3.2 CO Oxidation on Sulfur-Covered Pt

Fig. 2 shows a set of cyclic voltammograms for solution CO oxidation on Pt electrodes covered with various amounts of S obtained in CO-saturated 0.1
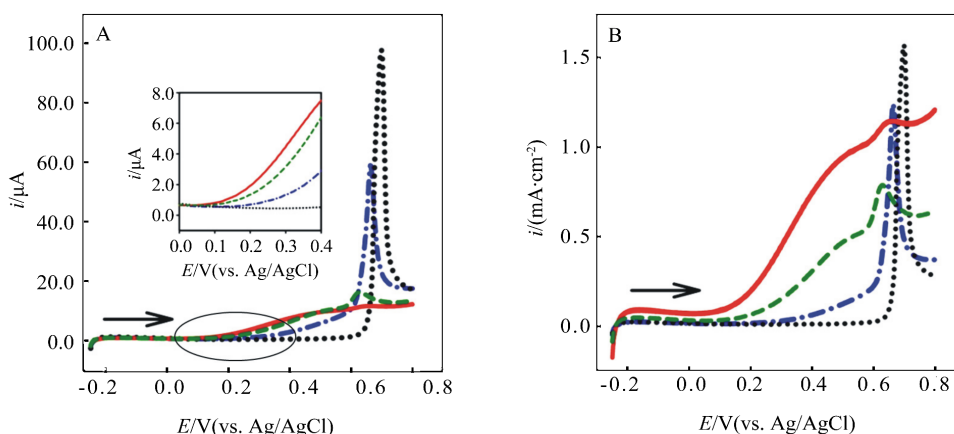
Fig. 2 Anodic segments of cyclic voltammogram of solution CO oxidation on Pt electrodes covered with various amounts of sulfur recorded in CO-saturated 0.1 mol·L^{-1} HClO$_4$. The CVs are plotted in current (A) and current density (B) forms. The inset in (A) is an enlargement of the portion marked by the circle. The relative sulfur coverage X_S are: solid: 0.86; dash: 0.63; dash-dotted: 0.24; dotted: 0. Scan rate: 0.1 V·s^{-1}. The arrow indicates the scan direction.

mol·L^{-1} HClO$_4$. They are plotted in both current and current density forms. For clarity, only the anodic segments are shown. CO was introduced by purging the solution with the gas for 5 min. To ensure the CO concentration is largely unchanged during the experiment, the solution was blanketed with CO by flowing the gas above the solution. Current density is expressed in terms of the surface area available for CO adsorption, which was calculated by using the charges for hydrogen desorption from S-covered surfaces. This practice is justified by the observation that the number of adsorbed CO (CO$_{ads}$) blocked by S$_{ads}$ is nearly the same as that of H$_{ads}$ (vide infra). The relative sulfur coverage was obtained as described above. It is evident from Fig. 2 that the onset potential for solution CO oxidation shifts to more negative values with increasing amounts of sulfur on the surface. In addition, the shape of the voltammogram changes significantly with sulfur coverage. At low sulfur coverages, the voltammogram largely retains the peak shape with a pre-wave; at high sulfur coverages, the pre-wave becomes larger and eventually develops as the major component. These observations are in agreement with those reported by others[21, 23-24].

    To make a more quantitative assessment of the S$_{ads}$ effect on the solution CO oxidation, the onset

potential difference (ΔE), defined as the potential difference at a current equal to 5% of the CO oxidation peak current on the clean Pt surface, was measured and plotted as a function of the X_S (Fig. 3). The ΔE increases sharply with the amount of sulfur on the surface and approaches a plateau near X_S = 0.65. This observation is similar to that reported by Watanabe and Motoo[23-24]. As stated above, higher coverage of S$_{ads}$ ($\theta_S > 0.3$) can be obtained by increasing the sulfide concentration or the potential
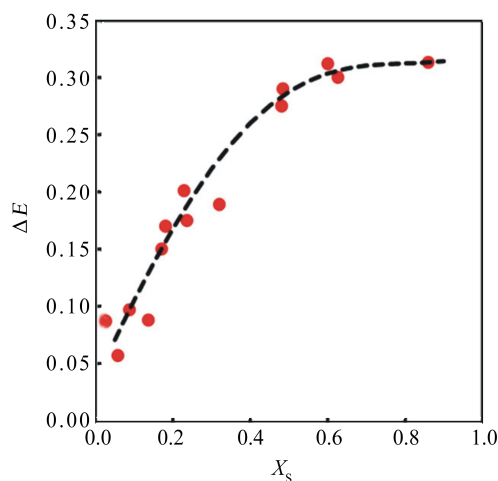

Fig. 3 The onset potential difference of solution CO oxidation on clean and S-covered Pt plotted against the relative sulfur coverage (the dash curve serves as a guide to the eye).

at which the sulfur layer is formed. However, at these coverages CO oxidation is completely blocked by adsorbed sulfur.

To understand the sulfur effect on the solution CO oxidation, we examined the electrooxidation of adsorbed CO (CO_{ads}) on sulfur-covered Pt. The general procedure of the experiment entails recording the CO stripping voltammogram on a clean Pt electrode, followed by CO stripping on the same electrode, but covered with various amounts of sulfur. This practice is necessary for minimizing the effects from the variation of the surface structure from trial to trial due to the polycrystalline nature of the surface. Fig. 4 shows a representative pair of cyclic voltammograms of irreversibly adsorbed CO oxidation on Pt electrodes with different X_S. The CO adlayer was formed by sequentially purging the solution with CO for 5 min and N_2 for 10 min while the electrode potential was held at 0.0 V. Interestingly, the potential shift of the adsorbed CO oxidation is very different from that of the solution CO: at X_S below 0.3, the shift is negative; above this value, the change is positive and larger at higher X_S. Nevertheless, the potential shift is small, typically between 30 mV and -40 mV. This CO oxidation peak potential shift is not due to the variation of the polycrystalline structure of the surface, since the CO oxida-

tion potential was compared on the same electrode before and after the S adsorption. This observation is different from those reported by Park et al. that show CO stripping peak potential moves to more negative values as the sulfur coverage increases[26]. This difference likely arises from the use of nanoparticles and the presence of the Nafion binders in their studies. Other studies have shown that anion adsorption, such as chloride or bromide, typically yields higher CO oxidation potential as compared to the clean surface, albeit the coverage of the anion is typically high at the CO oxidation potential because it is present in the supporting electrolyte[36]. In the present case the S_{ads} is preformed and stable after CO is introduced into the solution free of sulfide, therefore the amount of Sads can be well controlled and systematically varied. In contrast, although the adlayer of halides can be retained after the electrode is removed from the solution containing the anions, the adsorbed halides will be partially or even completely replaced by CO depending on the potential, preventing the study of halide coverage dependence of the CO oxidation.

From the adsorbed CO oxidation charge, it is possible to estimate how many CO_{ads} are blocked by one S_{ads} by comparing the θ_S with the X_S evaluated from CO oxidation charge, which is denoted as X_S

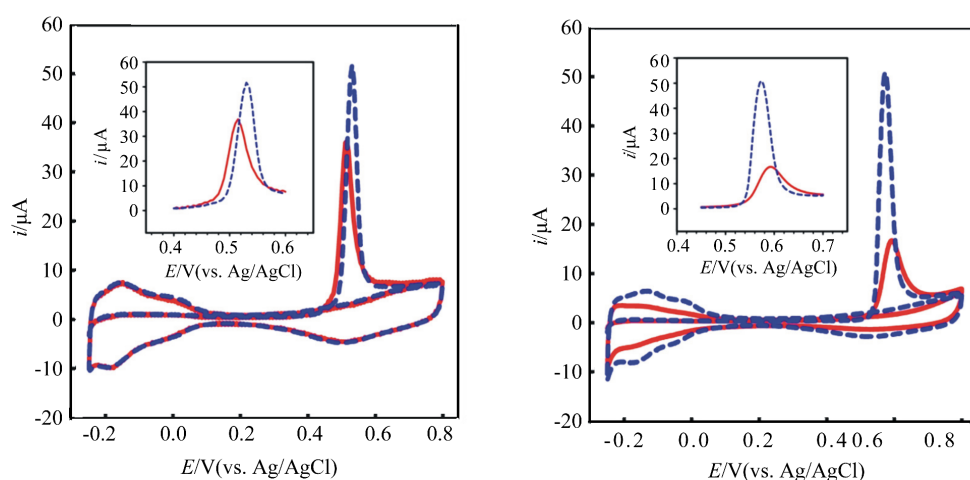Fig. 4 Cyclic voltammograms of irreversibly adsorbed CO oxidation on clean (dash traces) and sulfur covered (solid traces) Pt electrodes in 0.1 mol·L^{-1} HClO$_4$. The relative sulfur coverages X_S are: A. 0.09; B. 0.48. The insets are the enlargement of the peak section of the first anodic segment of the corresponding CVs, showing the peak potential shift of the adsorbed CO oxidation. Scan rate: 0.1 V·s^{-1}.

(CO), in a similar fashion to the procedure described above for X_S from Eqn. (1) (we will use $X_S(H)$ for this quantity when both are present). Alternatively, the same information can be obtained by comparing the $X_S(H)$ with the $X_S(CO)$. If the two are equal, the S_{ads} blocks the same amount of CO_{ads} as H_{ads} does. Displayed in Fig. 5 is a plot depicting the relationship between $X_S(H)$ and $X_S(CO)$. The $X_S(CO)$ was obtained in a similar manner to that described in Eqn. (1), except that the charge for CO oxidation was used in this case. The data points in Fig. 5 distribute very close to the unit slope line (the dash trace in Fig. 5), indicating that the $X_S(H)$ and $X_S(CO)$ are nearly the same. This suggests that the S_{ads} blocks the same number of H_{ads} and CO_{ads}, which is not unity as shown above.

3.3　Chronoamperometric Results of CO Oxidation

To reveal the mechanism behind the catalytic effect of the S_{ads} on the CO oxidation, chronoamperometry was also employed. The experiments were all conducted in a single-potential step fashion with an initial potential at 0.0 V and various final potentials. Both the solution and the adsorbed CO oxidation were examined. Since the catalytic effect for solution CO oxidation is most prominent at high X_S, we focus on the chronoamperometric studies in this X_S region for now. Fig. 6 shows a selective pair of current-time transient plots obtained on clean (dash-traces) and S-modified (solid traces) Pt electrodes. The X_S was fixed at 0.82. The initial potential was 0.0 V and the final potential was 0.40 V for solution CO and 0.45 V for adsorbed CO oxidation. The corresponding i-t transient obtained in 0.1 $mol \cdot L^{-1}$ $HClO_4$ without CO was used as the background and subtracted from each plot. For the solution CO oxidation, consistent with the cyclic voltammetric results, the steady state current on S-covered Pt is much higher than that on clean Pt electrode, as long as the final potential was kept below the take-off potential (around 0.6 V) of the CO oxidation on clean Pt. The i-t plot for the final potential in the range of
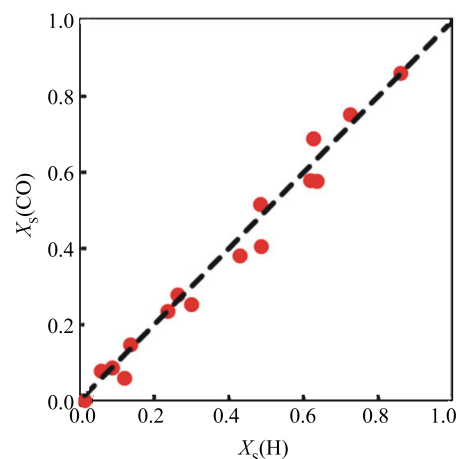

Fig. 5　Comparison of the relative sulfur coverage obtained from the H desorption charge, $X_S(H)$, with that from the adsorbed CO oxidation charge, $X_S(CO)$, on the same sulfur covered Pt electrode. The dash trace shows a unit slope line as a guide to the eye.

0.35 to 0.6 V has a very similar shape. Close inspection of Fig. 6A reveals that the oxidation current decays faster on the S-covered Pt at a shorter time (< 2 s), but at a longer time, the current decays more rapidly on the clean Pt (Fig. 6A, inset). This transition of current decay rate also occurs at other final potentials that are below the peak potential of CO oxidation on the clean surface. The above observations indicate that CO oxidation is more facile on the S-modified surface, leading to a larger current at lower overpotentials. It should be pointed out that the chronoamperometric results are plotted in the current-time format. Given that for S-modified Pt part of the surface is covered by S_{ads} and CO oxidation does not occur on these sites, the difference between S-covered and clean Pt electrodes will be even larger if the results were plotted in the current density (with respect to the Pt area available for CO adsorption) form.

For adsorbed CO oxidation, the current-time transient plot for S-covered Pt is drastically different from that of the clean Pt surface. On the clean Pt surface, the transient shows a current plateau at shorter times (< ~ 4 s) and followed by a current peak at about 6 s. The length of the plateau and the position of the peak current strongly depend on the
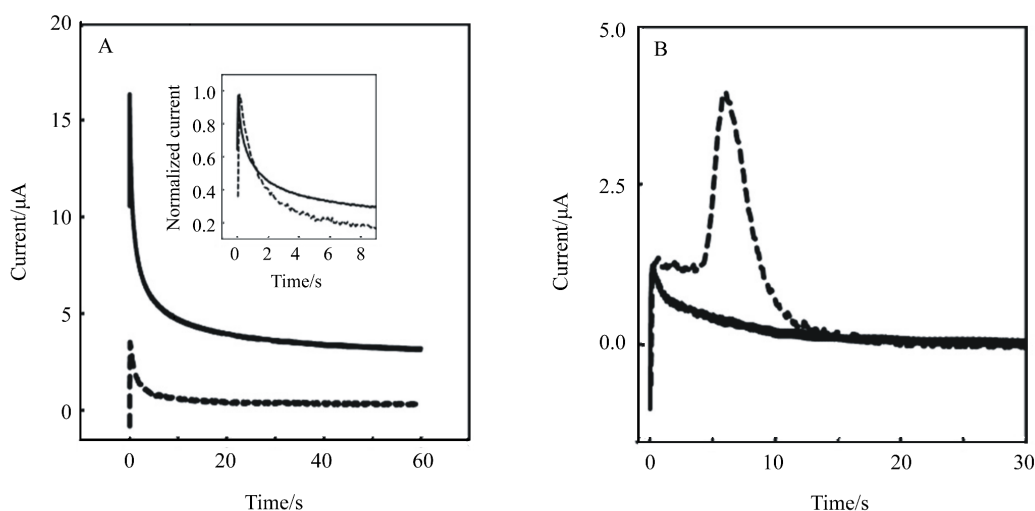
Fig. 6 Single potential step current-time transient plots for solution (A) and adsorbed (B) CO oxidation on Pt electrodes obtained in CO-saturated and N_2-purged 0.1 mol·L⁻¹ $HClO_4$, respectively. Initial potential: 0.0 V; final potential: A. 0.40 V; B. 0.45 V. Solid trace: S-covered Pt with X_S = 0.82. Dash trace: clean Pt. The inset in A shows the current-time transient in normalized current and a shorter time scale to demonstrate the current decay rate in the two cases.

final potential. The higher the final potential, the shorter the plateau, and the shorter time the peak appears. These results agree with those reported on Pt (111) and its vicinity step surfaces[37-39]. The plateau was attributed to the relaxation of the compact CO adlayer as a result of the oxidation of small amount of CO_{ads}. The appearance of the current peak can be explained by the Langmuir-Hinshelwood reaction mechanism[37-39]. The presence of S_{ads} changes the shape of the *i-t* plot significantly. Neither the plateau nor the peak remains. The current decays monotonically shortly after the potential step. This observation is similar to that obtained from CO_{ads} oxidation on Pt(111) surface with the CO coverage below 0.3[37], which is reasonable since at this sulfur coverage (X_S = 0.82), the θ_{CO} is below 0.2 (vide supra). However, it is different from that observed on Pt/C or Pt black where the current plateau and peak remain in the *i-t* plots, albeit at different times[26].

3.4 Surface-Enhanced Raman Spectra

Surface-enhanced Raman spectroscopy (SERS) with its capability of probing both the metal-adsorbate and the inter-adsorbate interactions provides an excellent means to explore the influence of S_{ads} on the Pt—CO bonding and the CO adlayer structure.

In addition, the applicability of SERS to a frequency region below 500 cm⁻¹ facilitates direct probing of the metal-adsorbate bonding change, which is of importance here. Shown in Fig. 7 is a representative set of SER spectra in the metal—CO and C—O stretching regions recorded in 0.1 mol·L⁻¹ $HClO_4$ with and without CO in the solution. Also shown is a spectrum on S-covered Pt taken before the introduction of CO into the solution for comparison. The spectra were obtained on Pt thin films deposited on a SERS-active Au substrate as described in the experimental section. All of the spectra were recorded with the electrode potential held at -0.2 V, and each spectrum covers a frequency region from 150 to 3000 cm⁻¹. For clarity, only the Pt-adsorbate stretching (150 to 750 cm⁻¹) and C—O stretching (1750 to 2150 cm⁻¹) regions are shown.

Starting from the lower frequency region (Fig. 7A), the two peaks at 398 and 488 cm⁻¹ in the spectrum a obtained on Pt without S_{ads} but with irreversibly adsorbed CO can be confidently assigned to the metal—CO stretching modes from CO adsorbed on two-fold and on-top sites, respectively[28, 40]. The spectrum obtained in CO-saturated 0.1 mol·L⁻¹ $HClO_4$ (not shown) resembles the spectrum a. Upon

adsorption of sulfur, the spectrum changes sharply: the 488 cm^{-1} band downshifts to 472 cm^{-1} and the 398 cm^{-1} peak is buried in a new feature with a main peak at 310 cm^{-1} and a shoulder at around 350 cm^{-1}. The new feature is similar to that obtained on S-covered Pt in 0.1 mol·L^{-1} HClO$_4$ without CO (Fig. 7A, spectrum d). Compared with the previous SERS study of sulfur adsorption on Pt [41-42], the main peak in the new feature can be assigned to the Pt-S stretching mode and the shoulder is likely from the S—S stretching of the trace amount of adventitious polysulfur, whose presence is further evident in the appearance of a weak feature at 475 cm^{-1} in the spectrum d (Fig. 7A)[43].

The intensity decrease in the Pt—CO stretching mode may arise from the lower CO coverage due to the S$_{ads}$ site blocking, although it could also arise from the non-uniformity of the SERS activity on the Pt. It should be pointed out that although the peak intensity in the SER spectrum varies from spot to spot on the surface, the Pt—CO stretching frequency only fluctuates 1 to 2 cm^{-1}. The redshift of the Pt—CO stretching band frequency is a direct indication of the weakening of the Pt—CO bond caused by the coadsorbed S[44]. Another significant spectral change can be seen by comparing the spectrum obtained on S-covered Pt in the CO saturated solution (Fig. 7A, spectrum b) with that acquired in the solution without CO in the solution (Fig. 7A, spectrum c). The intensity of the Pt—CO stretching band in spectrum b is significantly higher than that in spectrum c, although the Pt—CO stretching band position is largely the same. More importantly, the integrated band intensity ratio of the Pt—CO stretching mode to the Pt-S mode in spectrum b is nearly twice of that in the spectrum c, which suggests that the intensity change does not mainly come from the non-uniformity of the SERS activity on the surface. Rather, it arises from the loss of weakly adsorbed CO when the solution CO is removed. In contrast, on the Pt surface without sulfur, the Pt—CO stretching band intensity only changes slightly (typically less than 20%) when the dissolved CO is removed and the

laser was kept at the same spot on the surface. Interestingly, at this sulfur coverage, the Pt—CO does not change significantly after the solution CO is removed. However, at a lower sulfur coverage ($X_S =$ 0.5), the $\nu_{Pt\text{-}CO}$ increases from 476 cm^{-1} with CO in the solution to 482 cm^{-1} after the removal of solution CO, strongly supporting that there are weakly adsorbed CO which only exist with the presence of the solution CO. We pointed out that the decrease of $\nu_{Pt\text{-}CO}$ caused by the increase of CO coverage is much smaller, e.g. at saturated CO coverage the $\nu_{Pt\text{-}CO}$ is 488 cm^{-1} while it increases slightly to 490 cm^{-1} at $\theta_{CO} = 0.2$.

Now we turn to the higher frequency region (Fig. 7B). The spectrum from the Pt electrode without sulfur is similar to those reported before. The two bands centered at 1865 and 2076 cm^{-1} can be assigned to the C—O stretching mode from CO adsorbed on the bridging and atop sites, respectively[28, 40]. The spectral change after sulfur adsorption is not as prominent as in the Pt-adsorbate stretching region. A noticeable change is the decrease of the band intensity in both C—O stretching modes upon sulfur adsorption. As in the lower frequency region, this is likely due to the lower CO coverage arising from S$_{ads}$ physically blocking the available sites. Interestingly, the intensity of both C—O stretching bands decreases to the same extent, as the band intensity ratio before and after sulfur adsorption remains the same, indicating S$_{ads}$ equally blocks the atop and bridging CO$_{ads}$. This observation is different from a recent surface enhanced IR absorption spectroscopic study on S-modified Pt/C, in which the intensity of bridging CO$_{ads}$ decreases more than that of the atop CO$_{ads}$[26]. Consistent with the changes in the lower frequency region for the S-covered Pt surface, the removal of solution CO further decreases the band intensity of the C—O stretching modes (down about 50%), confirming the desorption of the weakly adsorbed CO. The intensity decrease is roughly proportional to the amount of CO. The frequency change for the CO modes is small, most notable is the slight redshift of the atop CO upon removal of the solution CO,
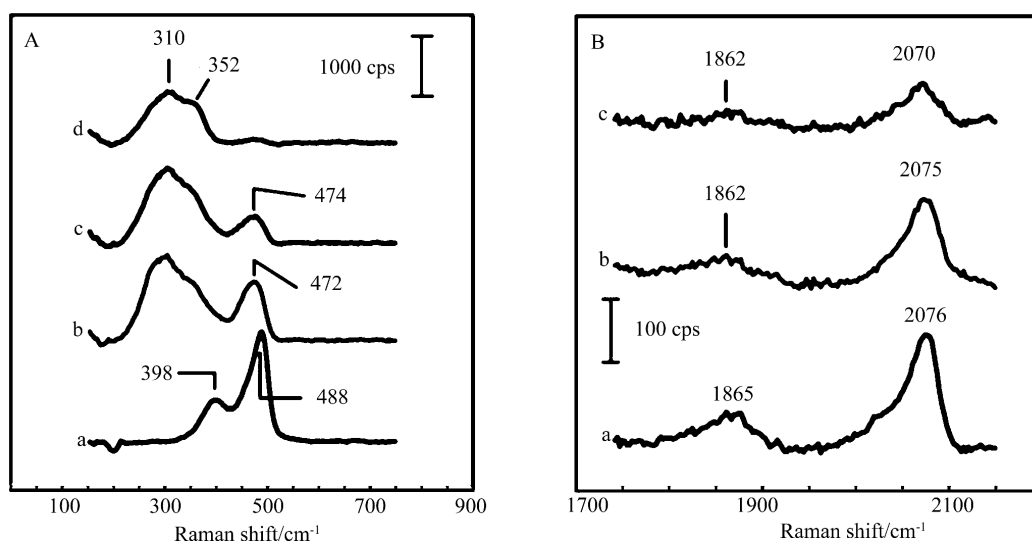
Fig. 7 SER spectra in metal-adsorbate (A) and C—O stretching (B) frequency regions obtained in (a, c, d) 0.1 mol·L⁻¹ HClO₄ and (b) CO-saturated 0.1 mol·L⁻¹ HClO₄ at -0.2 V. Spectrum a was obtained before and spectra b, c, d after S adsorption. Spectrum acquisition time: 30 s. Relative sulfur coverage X_S : 0.85.

which could be from stronger CO—Pt bonding and/or a weaker dynamic dipole-dipole coupling due to a smaller CO coverage[45-46].
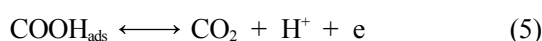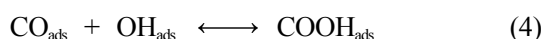
3.5 Solution pH Dependence of Sulfur Promoting Effect on the CO Electrooxidation

To shed light on the sulfur promoting effect on the CO electrooxidation at Pt electrodes, we examined further the solution pH dependence of the CO oxidation onset potential. The solutions with different pHs were prepared as described in the experimental section. The sulfur effect on the CO oxidation was measured by the onset potential difference between clean and sulfur covered Pt electrodes. The onset potential is again taken as the potential at 5% of the CO oxidation peak current on the S-free Pt. Fig. 8 shows a plot of the onset potential difference (ΔE) as a function of the solution pH. Only the data points with an X_S above 0.6 are included in the plot. As shown in Fig. 3, in this X_S range, the ΔE is largely the same at a fixed solution pH. Therefore the data points reflect the effect of solution pH, not the X_S. The error bar represents the range of ΔE obtained at each pH and each data point is an average of results from at least three separate measurements. From Fig.

8, it is clearly evident that the ΔE is significantly larger in the acidic media than in the neutral or basic solutions. This pH dependence is different from that reported by Watanabe and Motoo, who found the ΔE is smallest at pH7 and larger in both the basic and acidic media[24]. The anion specific adsorption in solutions with pH higher than 3 plays a minor role in the ΔE, as evident by the similar ΔE_S observed in both sulfuric acid and perchloric acid solutions.

4 Discussions

Of central interest here is to understand the catalytic effects of S_{ads} on the electrooxidation of carbon monoxide. The electrooxidation of CO on Pt has been extensively studied both theoretically and experimentally. It is generally accepted that the reaction proceeds through a Langmuir-Hinshelwood mechanism, which can be represented by the following reaction steps in an acidic medium[39, 47] :

$$H_2O \longleftrightarrow OH_{ads} + H^+ + e \qquad (3)$$

$$CO_{ads} + OH_{ads} \longleftrightarrow COOH_{ads} \qquad (4)$$

$$COOH_{ads} \longleftrightarrow CO_2 + H^+ + e \qquad (5)$$

The second step is generally considered as the rate determining process. The reaction rate is therefore proportional to both the CO and OH coverages.
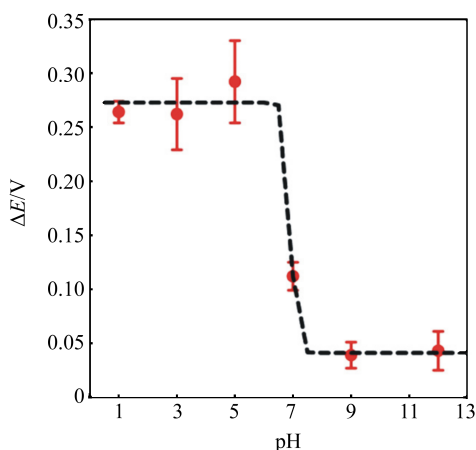
Fig. 8 The onset potential difference of the solution CO oxidation on clean and S-covered Pt electrodes as a function of the solution pH. The dash curve serves only as a guide to the eye.

Depending on whether the CO_{ads} and OH_{ads} form a well mixed adlayer, there are two extreme cases-mean field approximation model and nucleation-and-growth kinetics [37-39, 47-48]. If the CO_{ads} and OH_{ads} form a well mixed layer or the diffusion of the CO_{ads} or OH_{ads} on the surface is faster than reaction (4), the reaction kinetics can well be described by the mean-field approximation. If the CO_{ads} diffusion is slow, the nucleation-and-growth approach is a better description. Through a series of studies on Pt (111) and its vicinity step surfaces, Lebedeva et al. concluded that CO_{ads} diffusion on Pt surfaces is fast, and the mean-field approximation is a better model for the system[37-39].

In the present case, the addition of sulfur on the Pt surface has several significant effects on the CO adsorption. From photoemission spectroscopic experiments and ab initio self-consistent field calculations, it is found that S_{ads} decreases Pt 5d orbital occupancy significantly[18]. This will increase the CO 5σ to Pt d donation but lower the extent of the metal d to CO 2π* back donation, which affect the Pt—CO bonding[44, 49]. More importantly, the repulsive interaction between CO and S weakens the CO—Pt bonding. In agreement with these, in the ultra high vacuum environment, the thermal desorption spectroscopic (TDS) studies indeed show that CO des-

orbs at lower temperatures on S-covered Pt as compared to the clean surface[5, 7-8, 14, 50]. The binding energy of CO adsorption on terminal sites was lowered by more than 30 kJ·mol^{-1}[7]. In the present study, the SER spectra show that the coadsorbed S redshifts the Pt—CO stretching frequency by more than 15 cm^{-1}. The change of the Pt—CO stretching frequency, rather than the C—O stretching, is a direct indication of Pt—CO bonding change, as shown by density functional theorycalculation [44, 49]. The redshift of Pt—CO stretching frequency therefore indicates the weakening of Pt—CO bond. The weaker CO—Pt bonding facilitates the CO oxidation.

Why, then, only the solution CO oxidation shows a strong S_{ads} effect? The SER spectra show that after removal of CO from solution, the intensity of vibrational bands from CO_{ads} decreases, which indicates the loss of CO_{ads}. These weakly adsorbed CO are likely to be oxidized at more negative potentials, similar to the pre-peak observed at CO oxidation on Pt(111)[51]. In other words, there are sites that are more active toward CO oxidation on the surface and these sites are created by the presence of S_{ads}. In agreement with the SERS results, the measured X_s is several times that of θ_S, suggesting that without dissolved CO in the solution there are sites that are not occupied by CO_{ads} or S_{ads}. The coadsorption of S and CO has been shown by using scanning tunneling microscopy (STM) and low energy electron diffraction (LEED) in the UHV to form segregated CO and S islands on Pt(111) due to the repulsive interaction between the two adsorbates[19, 52-54]. At the boundary of the S islands, CO adsorption is likely to be weaker and these surface sites are likely to be responsible for the observed low overpotential of solution CO oxidation. In the presence of CO in the solution, there is a continuous supply of CO to the more active sites. When the solution CO is removed, these weakly adsorbed CO desorb, leaving the more active sites free of CO_{ads}. The CO_{ads} remaining on the surface do not diffuse to these more active sites or the diffusion is very slow due to the repulsion of the CO_{ads} and S_{ads}. Consistent with this picture, it has

been shown in UHV that S_{ads} strongly suppresses the CO diffusion on Ni(110)[55].

The pH-dependent ΔE shown in Fig. 8 can be understood in terms of the competitive adsorption of CO and OH⁻ at these more active sites. At high pH, the adsorption of OH⁻ at the sites near S_{ads} blocks the CO from these sites therefore the promotion effect is much smaller. At low pH, OH⁻ adsorption cannot compete with the CO adsorption.

The observed $\nu_{Pt\text{-}CO}$ blueshift on S-covered Pt upon removal of solution CO supports the notion that desorption of weakly adsorbed CO does occur, leaving behind more strongly bound CO. Compared with the S-free surface, the Pt—CO obtained either with or without CO in the solution is lower on the S-covered Pt, suggesting that in addition to the weakening of the Pt—CO bond at sites next to the S_{ads}, on which the CO_{ads} desorb after the removal of the solution CO, S_{ads} reduces the overall Pt—CO bond strength. This observation suggests that S_{ads} has both short and long range effects on the Pt—CO bond.

For the oxidation of irreversibly adsorbed CO, the presence of a small amount of S_{ads} ($X_S < 0.3$, roughly equivalent to $\theta_S = 0.1$) decreases the peak potential. However, if the X_S is higher, the peak potential is more positive. This may be understood in terms of the CO adlayer structure change with the presence of S_{ads} and the S_{ads} distribution. At low X_S, S_{ads} decorates in the CO adlayer and forms an intermixed adlayer. The CO_{ads} does not need to travel a long distance to react with OH_{ads} and more importantly the diffusion of CO_{ads} is not significantly inhibited by S_{ads} as compared to when S_{ads} form islands at higher X_S, therefore the reaction is facile. At higher X_S, S_{ads} and CO_{ads} may form segregate islands, the CO_{ads} diffusion is significantly slowed down and the reaction is therefore retarded. Several lines of evidence support the slow CO diffusion. From the CO stripping voltammogram (Fig. 4B), the CO_{ads} oxidation peak is much broader on S-covered Pt than on the unmodified surfaces. From the chronoamperograms in Fig. 6B, the CO oxidation plateau and peak

disappear on S-modified Pt. These observations are characteristics of slower CO diffusion[38, 56]. In addition, after removal of dissolved CO from the solution, the C—O stretching frequency which is very sensitive to the CO coverage only redshifted 5 cm⁻¹, suggesting after removal of solution phase CO the strongly adsorbed CO do not diffuse to the vacant sites and the CO island largely remain intact. However, in either cases, energetically the CO adlayer is more reactive than the clean surface because the coadsorption of sulfur weakens the Pt—CO bond, but kinetically the CO surface diffusion rate determines where the current peak appears.

It has been reported that the presence of acetonitrile (< 0.01 mol·L⁻¹) in the electrolyte also promotes solution CO oxidation, but strongly inhibited adsorbed CO oxidation[57]. This observation was explained partly by the so-called "third-body effect", in which the adsorbed acetonitrile blocks the surface sites that are less active for CO oxidation, leaving behind the more active sites[57]. While the "third body effect" can explain the weakening of the Pt—CO bond in the present case, it cannot account for the enhancement of CO oxidation. Had the more active sites been on the surface before S adsorption, solution CO oxidation current would be observable at low overpotentials on S-free Pt. In addition, adsorbed halides, which would have a third body effect similar to that of S_{ads}, inhibit solution CO oxidation, strongly against the third body effect being the main mechanism for the enhancement of solution CO oxidation by S_{ads}[36].

5 Conclusions

Sulfur adlayer on Pt up to a relative coverage of $X_S = 0.9$ can be obtained by holding the electrode potential at -0.6 V in dilute Na₂S solutions. The obtained S adlayer is stable in the potential range from -0.25 to 0.8 V in 0.1 mol·L⁻¹ HClO₄. The effect of S_{ads} on the carbon monoxide electrooxidation was examined. By using cyclic voltammetry and chronoamperometry, we have demonstrated that Pt electrodes modified with a small amount of sulfur can significantly increase the surface reactivity to-

ward CO oxidation. For the solution CO oxidation, the onset potential of the reaction shifts to the negative direction up to over 300 mV, and the extent of the potential shift increases with a relative sulfur coverage up to about 0.9. For adsorbed CO, at low sulfur coverage ($X_S < 0.3$), the oxidation peak potential is about 40 mV negative to that of the corresponding clean Pt. However, at higher coverages, the peak potential is about 30 mV more positive. Surface-enhanced Raman spectra show that the adsorption of sulfur weakens the overall Pt—CO bond, which is a long range effect. In addition, the Pt—CO bonding strength for CO_{ads} near the S_{ads} is reduced to an even larger extent; the adsorption becomes reversible-the CO_{ads} desorb after the removal of dissolved CO from the solution. This is probably a short range effect. The effects of S_{ads} on the adsorbed and solution phase CO oxidation on Pt are a result of different interplaying effects. On one hand, the repulsive electrostatic interaction between CO_{ads} and S_{ads}, as well as the decrease of Pt d band occupancy by S_{ads}, weakens the Pt—CO bond. On the other hand, S_{ads} hinders the CO_{ads} diffusion to the more active sites.

Although the use of polycrystalline Pt in the present study hinders a more quantitative analysis of the adsorbed S effects on the reaction, a qualitative understanding of the S_{ads} catalytic effect is nonetheless achieved. It remains to examine how the catalytic effect depends on the surface crystal orientation. In addition, preliminary results from different metal surfaces suggest that the catalytic effect is metal dependent, which is yet to be understood. These studies will shed further lights on the effects of S_{ads} on the CO oxidation.

Acknowledgement

Supporting Information Available

The supporting information is available free of charge via the internet at http://electrochem.xmu.edu.cn.

References:

[1] Somorjai G A. Introduction to surface chemistry and catalysis[M]. New York, Wiley: 1994.

[2] Wimmer E, Fu C L, Freeman A. J. Catalytic promotion and poisoning—all-electron local-density-functional theory of CO on Ni(001) surfaces coadsorbed with K or S[J]. Physical Review Letters, 1985, 55 (23): 2618-2621.

[3] Feibelman P J, Hamann D R. Modification of transition metal electronic structure by P, S, Cl, and Li Adatoms[J]. Surface Science, 1985, 149: 48-66.

[4] Garfunkel E L, Farias M H, Somorjai G A. The modification of benzene and carbon-monoxide adsorption on Pt(111) by the coadsorption of potassium or sulfur[J]. Journal of the American Chemical Society, 1985, 107 (2): 349-353.

[5] Gdowski G E, Madix R J. The effect of sulfur on CO adsorption desorption on Pt(S)-9(111) × (100)[J]. Surface Science, 1982, 115(3): 524-540.

[6] Jorgensen S W, Madix R J. Steric and electronic effects of sulfur on CO adsorbed on Pd(100)[J]. Surface Science, 1985, 163 (1): 19-38.

[7] Kiskinova M, Szabo A, Yates J T. CO adsorption on Pt(111) modified with sulfur[J]. Journal of Chemical Physics, 1988, 89 (12): 7599-7608.

[8] Lanzillotto A M, Bernasek S L. The effect of the sulfur induced reconstruction of the Pt(S)-6(111) × (100) surface on CO adsorption[J]. Surface Science, 1986, 175(1): 45-54.

[9] Protopopoff E, Marcus P. Coadsorption of sulphur and hydrogen on Pt(111) studied by radiotracer and electrochemical techniques[J]. Surface Science, 1986, 169: L237-L244.

[10] Protopopoff E, Marcus P. Effect of chemisorbed sulfur on the electrochemical hydrogen adsorption and recombination reactions on Pt (111) [J]. Journal of Vacuum Science and Technology A, 1987, 5 (4): 944-947.

[11] Protopopoff E, Marcus P. Potential-pH diagrams for sulfur and hydroxyl adsorbed on copper surfaces in water containing sulfides, sulfites or thiosulfates[J]. Corrosion Science, 2003, 45(6): 1191-1201.

[12] Sung Y E, Chrzanowski W, Wieckowski A, et al. Coverage evolution of sulfur on Pt (111) electrodes: From compressed overlayers to well-defined islands[J]. Electrochimica Acta, 1998, 44(6/7): 1019-1030.

[13] Sung Y E, Chrzanowski W, Zolfaghari, A, et al. Structure of chemisorbed sulfur on a Pt(111) electrode[J].

Journal of the American Chemical Society, 1997, 119 (1): 194-200.

[14] Thomas V D, Schwank J W, Gland J L. Carbon monoxide desorption from platinum chemically modified by sulfur[J]. Surface Science, 2000, 464(2/3): 153-164.

[15] Zolfaghari A, Jerkiewicz G, Chrzanowski W, et al. Energetics of the underpotential deposition of hydrogen on platinum electrodes ii. Presence of coadsorbed sulfur[J]. Journal of the Electrochemical Society, 1999, 146(11): 4158-4165.

[16] Rodriguez J A, Chaturvedi S, Jirsak T. The bonding of sulfur to Pd surfaces: Photoemission and molecular orbital studies[J]. Chemical Physics Letters, 1998, 296 (3/4): 421-428.

[17] Rodriguez J A, Dvorak J, Jirsak T, et al. Coverage effects and the nature of the metal-sulfur bond in S/Au (111): High resolution photoemission and density-functional studies[J]. Journal of the American Chemical Society, 2003, 125(1): 276-285.

[18] Rodriguez J A, Kuhn M, Hrbeck J. The bonding of sulfur to a Pt(111) surface: Photoemission and molecular orbital studies[J]. Chemical Physics Letters, 1996, 251 (1/2): 13-19.

[19] Zaera F, Salmeron M. Coadsorption of sulfur and carbon monoxide on platinum single crystal surfaces studied by scanning tunneling microscopy[J]. Langmuir, 1998, 14(6): 1312-1319.

[20] Binder H, Kohling A, Sandstede G. Acceleration by adsorbed sulphur and selenium of the electrochemical oxidation of formic acid on platinum catalyst[J]. Nature, 1967, 214: 268-269.

[21] Binder H, Kohling A, Sandstede G. The anodic oxidation of carbon monoxide and formic acid on platinum covered with sulfur[M]//Baker B S, Ed. Fuel cell systems II. Washington, D.C.: American Chemical Society. 1969.

[22] Contractor A Q, Lal H. Formic acid oxidation at platinized platinum electrodes part V. A further study of catalytic effect of pre-adsorbed sulfur[J]. Journal of Electroanalytical Chemistry, 1979, 103(1): 103-117.

[23] Watanabe M, Motoo S. Electrocatalysis by Ad-atoms part XVI enhancement of carbon monoxide oxidation on platinum electrode in acid solution by the VIth Ad-atoms[J]. Journal of Electroanalytical Chemistry, 1985, 194(2): 275-278.

[24] Watanabe M, Motoo S. Electrocatalysis by Ad-atoms part XV. Enhancement of co oxidation on platinum by the electronegativity of Ad-atoms[J]. Journal of Electro-

analytical Chemistry, 1985, 194: 261-274.

[25] Loucka T. Adsorption and oxidation of organic compounds on a platinum electrode partly covered by adsorbed sulphur[J]. Journal of Electroanalytical Chemistry, 1972, 36: 355.

[26] Park I S, Chen D J, Atienza D O, et al. Enhanced CO monolayer electro-oxidation reaction on sulfide-adsorbed Pt nanoparticles: A combined electrochemical and *in situ* ATR-SEIRAS spectroscopic study[J]. Catalysis Today, 2012, http://dx.doi.org/10.1016/j.cattod.2012.05.045.

[27] Weaver M J, Zou S. Z, Chan H Y H. The new interfacial ubiquity of surface-enhanced raman spectroscopy [J]. Analytical Chemistry, 2000, 72(1): 38A-47A.

[28] Zou S Z, Weaver M J. Surface-enhanced Raman scattering an uniform transition metal films: Toward a versatile adsorbate vibrational strategy for solid-nonvacuum interfaces?[J]. Analytical Chemistry, 1998, 70(11): 2387-2395.

[29] Zou S Z, Williams C T, Chen E K Y, et al. Probing molecular vibrations at catalytically significant interfaces: A new ubiquity of surface-enhanced Raman scattering[J]. Journal of the American Chemical Society, 1998, 120(15): 3811-3812.

[30] Zou S Z, Williams C T, Chen E K Y, et al. Surface-enhanced Raman scattering as a ubiquitous vibrational probe of transition-metal interfaces: Benzene and related chemisorbates on palladium and rhodium in aqueous solution[J]. Journal of Physical Chemistry B, 1998, 102 (45): 9039-9049.

[31] Gao P, Gosztola D, Leung L W H, et al. Surface-enhanced Raman-scattering at gold electrodes—dependence on electrochemical pretreatment conditions and comparisons with silver[J]. Journal of Electroanalytical Chemistry, 1987, 233(1/2): 211-222.

[32] Mrozek M F, Xie Y, Weaver M J. Surface-enhanced Raman scattering on uniform platinum-group overlayers: Preparation by redox replacement of underpotential-deposited metals on gold[J]. Analytical Chemistry, 2001, 73(24): 5953-5960.

[33] Park I S, Xu B, Atienza D O, et al. Chemical state of adsorbed sulfur on Pt nanoparticles[J]. ChemPhysChem, 2011, 12(4): 747-752.

[34] Batina N, McCargar J W, Salaita G N, et al. Structure and composition of Pt(111) and Pt(100) surfaces as a function of electrode potential in aqueous sulfide solutions[J]. Langmuir, 1989, 5(1): 123-128.

[35] Foresti M L, Innocenti M, Forni F, et al. Electrosorption

valency and partial charge transfer in halide and sulfide adsorption on Ag(111)[J]. Langmuir, 2001, 14(24): 7008-7016.

[36] Markovic N M, Lucas C A, Rodes A, et al. Surface electrochemistry of CO on Pt(111): Anion effects[J]. Surface Science, 2002, 499(2/3): L149-L158.

[37] Lebedeva N P, Koper M T M, Feliu J M. Mechanism and kinetics of the electrochemical CO adlayer oxidation on Pt(111)[J]. Journal of Electroanalytical Chemistry, 2002, 524: 242-521.

[38] Lebedeva N P, Koper M T M, Feliu J M, et al. Role of crystalline defects in electrocatalysis: Mechanism and kinetics of CO adlayer oxidation on stepped platinum electrodes[J]. Journal of Physical Chemistry B, 2002, 106(50): 12938-12947.

[39] Lebedeva N P, Koper M T M, Herrero E, et al. Cooxidation on stepped Pt$[n(111) \times (111)]$ electrodes[J]. Journal of Electroanalytical Chemistry, 2000, 487(1): 37-44.

[40] Zou S Z, Weaver M J. Potential-dependent metal-adsorbate stretching frequencies for carbon monoxide on transition-metal electrodes: Chemical bonding versus electrostatic field effects [J]. Journal of Physical Chemistry.1996, 100(10): 4237-4242.

[41] Xu B, Park I S, Li Y, et al. An in situ SERS investigation of the chemical states of sulfur species adsorbed onto Pt from different sulfur sources[J]. Journal of Electroanalytical Chemistry, 2011, 662(1): 52-56.

[42] Mrozek M F, Weaver M J. Periodic trends in monoatomic chemisorbate bonding on platinum-group and other noble-metal electrodes as probed by surface-enhanced raman spectroscopy[J]. Journal of the American Chemical Society, 2000, 122(1): 150-155.

[43] Gao X P, Zhang Y, Weaver M J. Adsorption and electrooxidative pathways for sulfide on gold as probed by real-time surface-enhanced raman-spectroscopy [J]. Langmuir, 1992, 8(2): 668-672.

[44] Koper M T M, van Santen R A, Wasileski S A, et al. Field-dependent chemisorption of carbon monoxide and nitric oxide on platinum-group (111) surfaces: Quantum chemical calculations compared with infrared spectroscopy at electrochemical and vacuum-based interfaces[J]. Journal of Chemical Physics, 2000, 113(10), 4392-4407.

[45] Tang C, Zou S, Severson M W, et al. Coverage-dependent infrared spectroscopy of carbon monoxide on Iridium(111) in aqueous solution: A benchmark comparison

between chemisorption in ordered electrochemical and ultrahigh-vacuum environments[J]. Journal of Physical Chemistry B, 1998, 102 (44): 8796-8806.

[46] Tang C, Zou S Z, Severson M W, et al. Infrared spectroscopy of mixed nitric-oxide-carbon-monoxide adlayers on ordered iridium(111) in aqueous solution: A model study of coadsorbate vibrational interactions[J]. Journal of Physical Chemistry B.1998, 102 (43): 8546-8556.

[47] Korzeniewski C, Kardash D. Use of a dynamic monte carlo simulation in the study of nucleation-and-growth models for CO electrochemical oxidation[J]. Journal of Physical Chemistry B, 2001, 105(37): 8663-8671.

[48] Love B, Lipkowski J. ACS Symposium Series [M]. 1988, 378: 484-496.

[49] Koper M T M. Combining experiment and theory for understanding electrocatalysis[J]. Journal of Electroanalytical Chemistry, 2005, 574(2), 375-386.

[50] Bonzel H P, Ku R. Adsorbate interactions on a Pt(110) surface. I. Sulfur and carbon monoxide[J]. Journal of Chemical Physics, 1973, 58(10): 4617-4623.

[51] Markovic N M, Grgur B N, Lucas C A, et al. Electrooxidation of CO and H_2/CO mixtures on Pt(111) in acid solutions [J]. Journal of Physical Chemistry B, 1999, 103 (3): 487-495.

[52] Batteas J D, Dunphy J C, Somorjai G A, et al. Coadsorbate induced reconstruction of a stepped Pt(111) surface by sulfur and CO: A novel surface restructuring mechanism observed by scanning tunneling microscopy [J]. Physical Review Letters, 1996, 77(3), 534-537.

[53] Dunphy J C, McIntyre B J, Gomez J, et al. Coadsorbate induced compression of sulfur overlayers on Re(0001) and Pt(111) by CO[J]. Journal of Chemical Physics. 1994, 100(8): 6092-6097.

[54] McIntyre B J, Salmeron M, Somorjai G A. An *in situ* STM determination of a kinetic pathway for the coadsorbate-induced compression of sulfur by CO on Pt(111) [J]. Surface Science, 1995, 323: 189-197.

[55] Xiao X D, Xie Y, Jakobsen C, et al. Impurity effect on surface diffusion: CO/S/Ni(110) [J]. Physical Review Letters, 1995, 74(19): 3860-3863.

[56] Saravanana C, Markovic N M, Head-Gordon M, et al. Stripping and bulk CO electro-oxidation at the Pt-electrode interface: Dynamic Monte Carlo simulations [J]. Journal of Chemical Physics, 2001, 114(14): 6404-6412.

[57] Xia X H, Vielstich W. Enhanced oxidation of carbon monoxide on platinum in $HClO_4$ via interaction with acetonitrile[J]. Electrochimica Acta, 1994, 39(1): 13-21.

一氧化碳在硫修饰铂电极上的吸附与电氧化研究

Mathew A. Mattox, Matthew W. Henney, Adam Johnson, Shouzhong Zou*

(迈阿密大学化学 & 生物化学系, 美国 俄亥俄州 45056)

摘要: 吸附硫通常被认为是表面化学反应毒物, 然而少量的硫能够增强铂的一氧化碳(CO)电氧化活性. 本文利用常规电化学手段及表面增强拉曼光谱研究了 CO 在硫修饰的铂表面的电氧化. 对于溶液中的 CO, 其在硫修饰铂电极上的起始氧化电位最多可以比非修饰电极负移超过 300 mV, 而且在硫覆盖度低于 0.6 的条件下电位负移量随覆盖度增加而增大. 这一电催化活性的增强也受溶液 pH 值的影响. 在低硫覆盖度(小于 0.3)下, 吸附态的 CO 电氧化峰值电位比非修饰铂电极负移约 40 mV. 然而, 在高硫覆盖度下, 其峰值电位比非修饰铂电极正移近 30 mV. 表面增强拉曼光谱显示共吸附硫使 Pt—CO 振动频率显著红移. 作者认为这些结果是由于吸附硫弱化 Pt—CO 键及阻化 CO 在铂表面的移动引起的.

关键词: 电氧化; 硫; 一氧化碳; 铂电极; 表面增强拉曼光谱